

## Minimizing Warpage for Macro-Size Fused Deposition Modeling Parts

Thanh Thuong Huynh<sup>1</sup>, Tien V. T. Nguyen<sup>2,3</sup>, Quoc Manh Nguyen<sup>4</sup> and Trieu Khoa Nguyen<sup>2,\*</sup>

<sup>1</sup>Department of Mechanical Engineering, Can Tho University, Campus II, Can Tho, Vietnam

<sup>2</sup>Faculty of Mechanical Technology, Industrial University of Ho Chi Minh City, Ho Chi Minh, 70000, Vietnam

<sup>3</sup>Mechanical Engineering Department, National Kaohsiung University of Science and Technology, Kaohsiung, 80778, Taiwan

<sup>4</sup>Faculty of Mechanical Engineering, Hung Yen University of Technology and Education, Hung Yen, 16000, Vietnam

\*Corresponding Author: Trieu Khoa Nguyen. Email: [nguyenkhoatrieu@iuh.edu.vn](mailto:nguyenkhoatrieu@iuh.edu.vn)

Received: 21 December 2020; Accepted: 22 February 2021

**Abstract:** In this study, we investigated warpage and corner lifting minimization for three-dimensional printed parts generated by macro-size fused deposition modeling (FDM). First, the reasons for warpage were theoretically elucidated. This approach revealed that the thermal deformation and differential volumetric shrinkage of the extruded molten plastic resulted in warpage of FDM parts. In addition, low adhesion between the deposited model and the heated or non-heated printing bed may intensify warpage further. As a next step, initial small-size and medium-size models were used to identify parameters to manage and minimize warpage in a way that would reduce material consumption and running time. Finally, a macro-size model was built to experimentally investigate and verify the technical solutions to minimize the warpage of FDM parts. In conclusion, an improved part with reduced warpage was efficiently produced after detailed consideration of thermal effects and adhesion force. Potential exists to widen the application scope of FDM technology in manufacturing for processes like thermoforming that involve mold core fabrication with heating. This technology, which has applications not only in mechanical engineering but also in related engineering fields, is convenient and could readily be applied to practical manufacturing industries.

**Keywords:** Fused deposition modeling; corner lifting; volumetric shrinkage; thermal deformation; acrylonitrile butadiene styrene filament

### 1 Introduction

Fused deposition modeling (FDM), which is a filament-based technology, has become a simple and useful tool for three-dimensional (3D) printing [1]. In FDM, the temperature of a thermoplastic filament is increased to its melting point and subsequently forced through a cylindrical spout following the layer-by-layer cross-section of the model. The technique has several advantages including low maintenance costs, absence of toxic materials, and low-temperature



This work is licensed under a Creative Commons Attribution 4.0 International License, which permits unrestricted use, distribution, and reproduction in any medium, provided the original work is properly cited.

operation. However, some of the most commonly observed disadvantages include bad surface roughness due to seam lines between layers and warpage or corner lifting phenomena. Many researchers have focused on numerical and experimental investigations of warpage. Numerical simulation of warpage was utilized to comprehend the interaction between process parameters and material properties [2]. The authors of this study concluded that an optimizing process must be performed to lessen internal stresses for the minimization of warpage. Wang et al. [3] concluded that the main reason for warpage was thermal stress due to temperature gradients. They built a mathematical function of the warpage to quantitatively analyze the relevant parameters, including the material linear shrinkage rate  $\alpha$ , the stacking section length  $L$ , the chamber temperature  $T_e$ , and the number  $n$  of deposition layers, as a scientific tool for controlling and fine-tuning the warpage. In addition to studies of thermal stresses, a coupled thermal and mechanical analysis was used to mimic the FDM process [4] where the agglomeration of residual stresses at the bottom area of the printing part was the main cause of warpage. The authors suggested that scan speed and layer thickness were the most important factors that affected warpage. Sood et al. [5] performed experimental studies on the impact of essential process parameters that included raster width, air gap, raster angle, part orientation, and layer thickness. They examined the influence of these parameters on dimensional accuracy. The authors proposed that the printing process must be based on optimal settings to enhance dimensional accuracy. In other investigations [6], the authors also examined printing parameters that enhanced the stress accumulation along the paths of deposition causing more warpage of parts. The functional relation between building parameters and strength (flexural, impact, and tensile) for the FDM process has also been constructed using the response surface method for the prediction of warpage. In addition, researchers [7] quantified experimentally the influences of geometric forms and process parameters on the distortion of printing parts having thick-and thin-wall characteristics. The authors determined that the internal thermal stress may combine with the mass distribution to have an impact on dimensional accuracy, which was an extremely important evaluation index. Other studies [8] showed that sufficiently high thermal differences might cause warpage of the final printing parts. The authors claimed that the thermal history [9–11] of the printed path was of significant importance because it was the greatest determining parameter in the bonding quality between adjacent paths of material. Furthermore, Chau et al. [12] concentrated on process parameter optimization [13–17]. Parameters such as extrusion velocity, line width compensation, filling speed, and layer thickness were chosen as control parameters (input variables), while dimensional error, warp distortion, and printing time were chosen as outcome responses (evaluation indicators). The optimal results [18,19] were validated by confirmation experiments utilizing the response surface method in conjunction with the fuzzy inference system. A study by Peng et al. [20] proposed that a slightly negative air gap setting and thermal gradients resulted in the distortion of the physical dimensions of the printing parts. A negative air gap or negative fiber-to-fiber gap [21,22] denotes that the distance between the centers of two adjacent deposited molten filaments is smaller than the setting value of the height of the layer. While many investigations of the surface quality in FDM technology were performed, a way to systematically overcome warpage was needed. Almost all previous investigations that dealt with the warpage problem were about processing parameters [23]. General investigation for all relevant processes including pre-processing and processing parameters is needed. An experimental investigation for elucidating the reasons for warpage and minimizing this phenomenon was therefore performed in the present study.

In the remainder of this paper, Section 2 introduces the materials and methods used in our study. Section 3 describes the main results and discussion for the experimental process. Finally, the conclusions are presented in Section 4.

## 2 Materials and Methods

### 2.1 Fused Deposition Modeling (FDM)

The FDM technology was developed in the late 1980s and was commercialized in the early 1990s [24,25]. It offers several advantages, including nontoxic materials, unlimited geometric complexity, use with many types of materials, short operation cycle, easy changes of material, low processing temperature, small-size equipment, and low maintenance expenses [20,26]. In a normal FDM process, the heated nozzle plastic melts and extrudes a plastic by following the layer-by-layer cross-section of the part, which results in various layers of combined little strands as shown in Fig. 1 [27]. Consequently, the final printed model is formed by a matrix of little strands with the exception of the peripheral shell. Therefore, the constructed part can be observed as a porous model.

The FDM process is a layered manufacturing technology. It builds the desired 3D models directly from the computer-aided design (CAD) files or stereo lithography (STL) file. Therefore, the main disadvantages of this technology are due to seam lines between every two nearby small strands. These seam lines inherently induce a low surface quality or may even cause a loosening of layer-layer adhesion. Another important drawback is due to the thermal conductivity for polymeric materials utilized in the FDM technology. Furthermore, the polymer FDM parts' ability to withstand low heat prevents the widespread utilization of the FDM process.

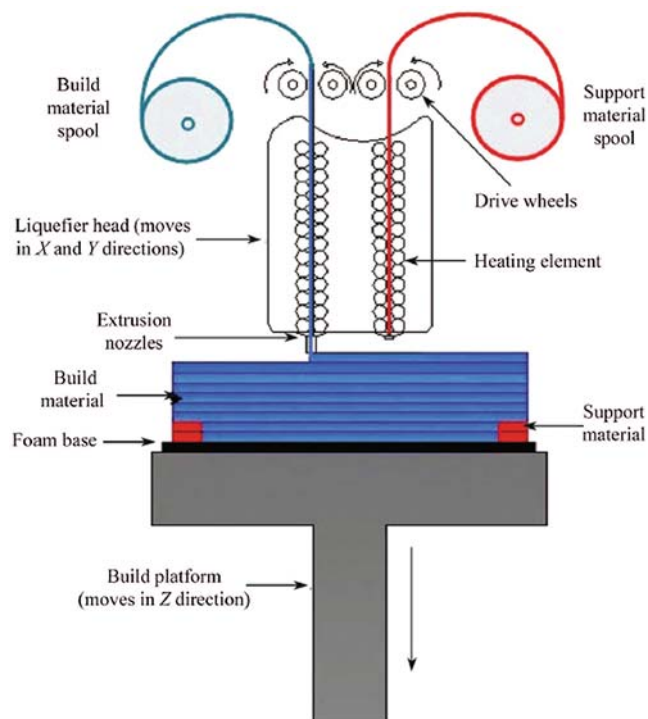


**Figure 1:** Illustration of a commonly used FDM technology [28]

## 2.2 Warpage in FDM

Thermal deformation and differential volumetric shrinkage of the extruded polymer melt mostly induce warpage in FDM models [29,30] just like the common warpage defects observed in injection molding technology. The inner core of the printed model usually has a greater temperature because of quicker cooling in the outermost shell or the peripheral layers as shown in Fig. 2. This imbalance in cooling induces inconsistent shrinkage, and therefore deformations lead to warpage or corner lifting. A loosening of adhesion between the built model and building bed may enhance the corner lifting or warpage more.

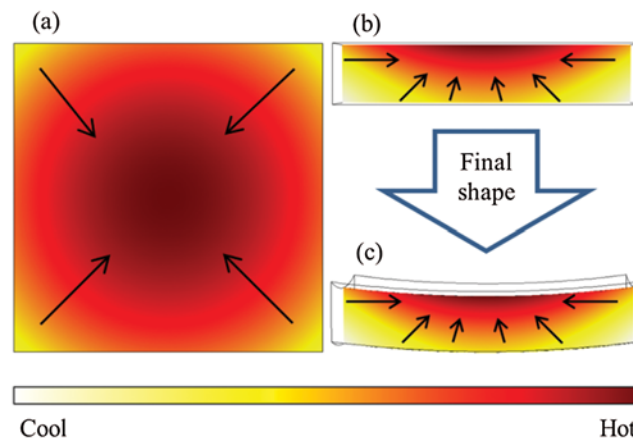


**Figure 2:** Corner-lifting or warpage phenomenon in FDM: (a) Top view of the FDM part, (b) side view of the FDM part, and (c) side view of the deformed model

## 2.3 Fabrication of Specimens

As a first step, 3D models were designed using a commercial CAD software program (Solid-Works). An initial small-size model was used to identify initial parameters. Medium-size model was used to reduce material consumption as well as running time. Minimizing corner lifting in the final large-size model was the target goal of this investigation as shown in Fig. 3. Next, the designed modeling 2D CAD sketches were converted to folders for differently formatted files (including STL) that are commonly utilized for 3D additive print. The STL files were then transformed into printable or buildable 3D files by splitting the designed parts into finite layers using the 3D printing software. The software also determined the appropriate deposition paths for the printing. The models were then printed out using ABS filaments on a commercial 3D printing machine (Cubicon Single) [30]. It should be noted that with an exact range of 0.025–0.6 mm, the utilized 3D printing machine resulted in somewhat poor printing quality. The models with the low surface-quality were purposely chosen to illustrate the performances of the proposed post-processing approach.

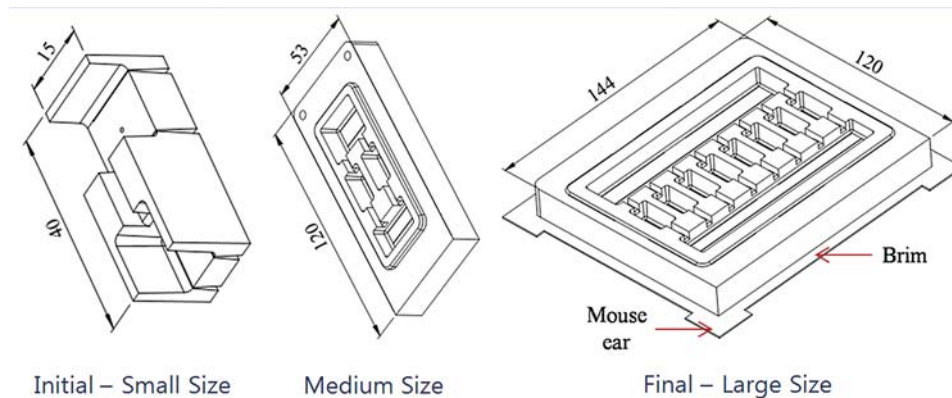


**Figure 3:** Three types of FDM specimens used in this study

### 3 Results and Discussions

In the pre-feasibility printings, corner lifting could be easily observed, even with the initial small-size samples. This defect prevented the 3D printing machine from being efficiently used as shown in Fig. 4.

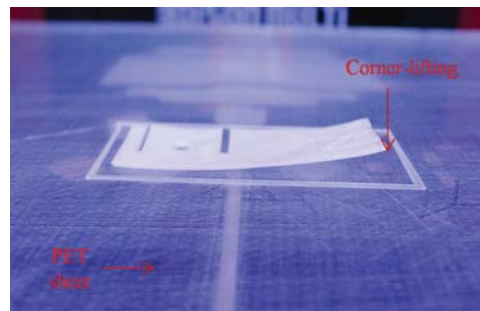


**Figure 4:** Corner-lifting/warping phenomenon in FDM

Hence, several pre-processing steps were carried out to efficiently enhance the stickiness between the printed model and the printing or building bed as follows: (i) The initial Z-height of the FDM equipment was carefully calibrated to print an initial layer sufficient for the extruded strand to cling onto the building bed with ease; (ii) the current building bed was covered by a polyimide tape with high heat resistance; (iii) the polyimide tape was painted using an ABS glue to form a thin ABS film to increase the stickiness of the extruded ABS strand onto the building bed as shown in Fig. 5; (iv) additional things were added to the model, for example, mouse ears and/or brims for better adhesion of the outermost layers and the corners to the printing bed; and (v) supplement drops of ABS glue were added between the mouse ears and/or brims to increase stickiness.

The relative parameters were also thoroughly handled during printing to miniaturize the thermal deformation and differential volumetric shrinkage as follows: (vi) The lowest possible printing or building temperature was set, which is needed for a reliable fabrication, but also generates good interlayer stickiness (250 °C for the current ABS wire); (vii) the part was printed at a low velocity (60 mm/s for the current case) for the built model to cool down evenly; (viii) the

building velocity was adjusted to the sole floor layer (first layer), which was slower in comparison to the cardinal printing velocity for increasing the stickiness of  $30 \text{ mm} \times \text{s}^{-1}$  for the current cases; and (ix) the printing bed temperature was controlled at  $110 \text{ }^\circ\text{C}$ , a little above the glass transition temperature of ABS polymeric material (about  $105 \text{ }^\circ\text{C}$ ), to let the fabricated model cool down more evenly.



**Figure 5:** The use of ABS glue on additional mouse ears

These nine important results served as the guidelines for us to utilize a 3D printing machine to develop a new type of mold core for processes incorporating heating such as thermoforming [31]. The impact of these nine results on the printing process is shown in Fig. 6. Previously, high warpage occurred during printing even with an initial small-size sample, despite the convenient costs, eco-friendliness, clean to use, and other advantages [32,33]. Now, more time was spent on printing because of the earlier mentioned nine actions. However, the better result showed that the time was worth it. The thick brim enlarged the sole layer, which was firmly stuck to the newly Kapton tape by adding ABS glue. It is worth noting that the brim can be easily removed after completing the printing process using a paper cutter. The brims, including the dried ABS glue, can be utilized as new ABS glue using acetone. The only disadvantage of the proposed sequence of steps was the damage to the Kapton tape due to high adhesion.

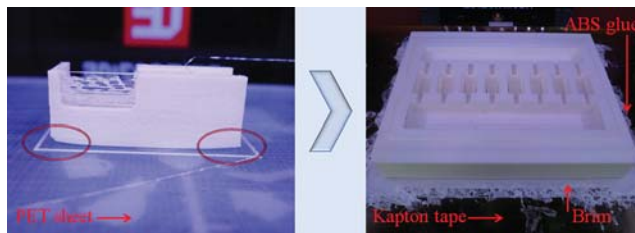


**Figure 6:** Two representative printed samples: Previous initial small-size sample with large corner lifting during printing, and better final large-size sample produced by utilizing preprocessing

The differences between setting parameters before and after improvement are shown in Tab. 1. It is worth noting that before improvement, the setting temperature values were the averages of the recommended ranges, while other settings were the same as those of Polylactic Acid (PLA) filaments.

The new model was produced based on the parameters shown in Tab. 1 and with consideration of the thermal problems and stickiness forces [34–37]. The new model part with diminished warpage was printed successfully as shown in Fig. 7. The additional components (including a



mouse-ear brim) were cut off without trouble after finishing the fabricating procedure. Consequently, using the proposed fabricating schematic diagram, the current FDM-printed models were fabricated adequately and did not require modification. It is worth noting that the values in the column “Values for typical samples” in Tab. 1 are the default values of the manufacturer of the printing machine. The values in the column “Values for improved samples” in Tab. 1, which include temperatures and printing speed, are those from the proposed nine steps mentioned above. A lower infill was chosen because less material led to a need for less shrinking of material. An infill of 60% was determined from preliminary experiments to be enough for the printed mold core to be utilized in the thermoforming apparatus.

**Table 1:** Parameters for 3D printer

Parameters	Units	Values for typical samples	Values for improved samples
Filling rate	%	90	60
Layer height	mm	0.2	0.2
Nozzle diameter	mm	0.4	0.4
Thickness of shell	mm	0.4	0.4
Top and bottom thickness	mm	0.6	0.6
Feed rate	%	97	97
Output speed	mm $\times$ s <sup>-1</sup>	80	60
Shell speed	mm $\times$ s <sup>-1</sup>	50	30
Floor layer speed	mm $\times$ s <sup>-1</sup>	50	20
Output temperature	°C	260	250
Heat bed temperature	°C	120	110
First layer thickness	mm	0.3	0.3

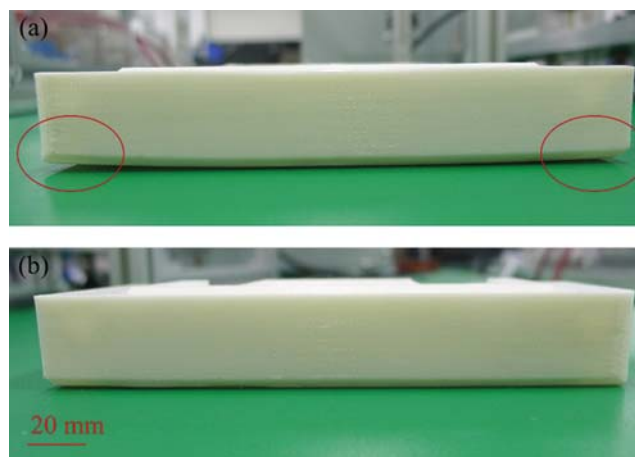


**Figure 7:** Two representative printed samples: (a) Previous sample with large corner lifting after printing, and (b) better sample printed by utilizing preprocessing

An additional benefit from the proposed sequence was the quality of the sole layer. It was improved significantly due to the gloss surface of the Kapton tape. The sole layers of the printed samples for the initial small-size parts are shown in Fig. 8 compared with a purchased PET sheet and new Kapton tape. The appearance of the sole layer is such that it does not significantly affect the functions of the sample as a mold core in a thermoforming process. This aesthetics can be a reason for the proposed sequence to be utilized in other processes.

It is worth noting that in the initial steps, using the default polyethylene terephthalate (PET) sheet for the printing bed, the machine could not finish the printing task using ABS filaments due to a poor adhesion problem. The warpage was around 3.7 mm using a polyimide film. The maximum warpage was around 0.8 mm after improvement, which is considered suitable for the use of a mold core in a thermoforming process [38,39].

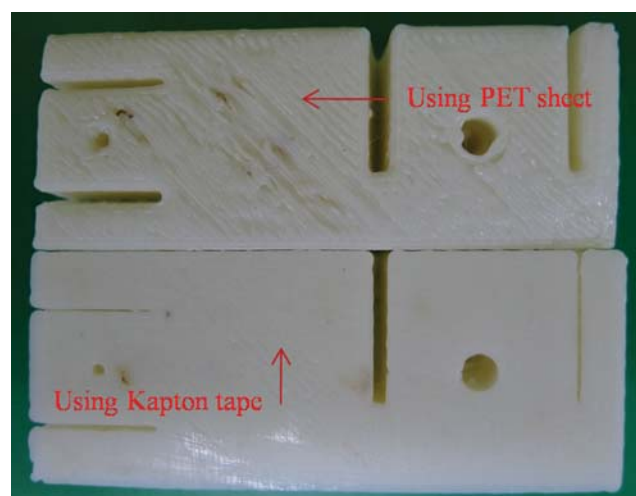


**Figure 8:** The sole layers of two printed samples: Previous sample with the PET sheet, and improved sample utilizing Kapton tape

#### 4 Concluding Remarks

In the present study, the warpage phenomenon, which is commonly observed in the FDM process for relatively large parts, was investigated. An improved part with reduced corner lifting was efficiently produced after consideration of thermal effects and adhesion force. Nine important results are highlighted that serve as guidelines to utilize a 3D printing machine to develop a new type of mold core for processes like thermoforming that incorporate heating. Our study differs from previous investigations in that it not only addresses the processing parameters of the warpage problem but more widely examines all relevant processes including pre-processing and processing parameters. After improvement, the maximum corner-lifting was around 0.8 mm, which is considered suitable for the use of a polymer mold core in a thermoforming process. Mouse ears brims, as well as additional ABS glue, can be removed easily after the printing process has been completed. The techniques used therefore did not affect the quality of the printed parts.



**Funding Statement:** The work presented in this study was orally presented at the first China–Vietnam symposium on precision manufacturing–CVPMS 2018, Industrial University of Ho Chi Minh City in Vietnam.

**Conflicts of Interest:** The authors declare that they have no conflicts of interest to report regarding the present study.

## References

- [1] T. K. Nguyen and B. K. Lee, “Minimization of corner lifting phenomena in fused deposition modeling,” in *Proc. KSMPE Annual Autumn Conf.*, Sacheon, Korea, pp. 78–85, 2015.
- [2] B. Wiedemann, K. H. Dusel and J. Eschl, “Investigation into the influence of material and process on part distortion,” *Rapid Prototyping Journal*, vol. 1995, no. 1, pp. 17–22, 1995.
- [3] T. M. Wang, J. T. Xi and Y. Jin, “A model research for prototype warp deformation in the FDM process,” *International Journal of Advanced Manufacturing Technology*, vol. 2007, no. 33, pp. 1087–1096, 2007.
- [4] Y. Zhang and K. Chou, “A parametric study of part distortions in fused deposition modelling using three-dimensional finite element analysis,” *Proceedings of the Institution of Mechanical Engineers, Part B: Journal of Engineering Manufacture*, vol. 2008, no. 222, pp. 959–968, 2008.
- [5] A. K. Sood, R. K. Ohdarand and S. S. Mahapatra, “Improving dimensional accuracy of fused deposition modelling processed part using grey Taguchi method,” *Materials & Design*, vol. 2009, no. 30, pp. 4243–4252, 2009.
- [6] S. K. Panda, S. Padhee, A. K. Sood and S. S. Mahapatra, “Optimization of fused deposition modelling (FDM) process parameters using bacterial foraging technique,” *Intelligent Information Management*, vol. 2009, no. 1, pp. 89–97, 2009.
- [7] S. Saqib and J. Urbanic, “An experimental study to determine geometric and dimensional accuracy impact factors for fused deposition modelled parts,” in *Enabling Manufacturing Competitiveness and Economic Sustainability*, Berlin, Germany, Berlin Heidelberg: Springer, pp.293–298, 2012.
- [8] B. N. Turner, R. Strong and S. A. Gold, “A review of melt extrusion additive manufacturing processes: Process design and modeling,” *Rapid Prototyping Journal*, vol. 2014, no. 20, pp. 192–204, 2014.
- [9] R. Yeu, N. Ra, S. Lee and Y. Nam, “Evaluation of pencil lead based electrodes for electrocardiogram monitoring in hot spring,” *Computers, Materials & Continua*, vol. 66, no. 2, pp. 1411–1425, 2021.
- [10] A. U. Rehman, F. Ali, A. Aamina, A. Imitaz, I. Khan *et al.*, “An unsteady oscillatory flow of generalized casson fluid with heat and mass transfer: A comparative fractional model,” *Computers, Materials & Continua*, vol. 66, no. 2, pp. 1445–1459, 2021.
- [11] A. U. Khan, N. Ahmed, S. T. Mohyud-Din, I. Khan, D. Baleanu *et al.*, “Al<sub>2</sub>O<sub>3</sub> and  $\gamma$ Al<sub>2</sub>O<sub>3</sub> nanomaterials based nanofluid models with surface diffusion: Applications for thermal performance in multiple engineering systems and industries,” *Computers, Materials & Continua*, vol. 66, no. 2, pp. 1563–1576, 2021.
- [12] N. L. Chau, T. P. Dao and V. T. T. Nguyen, “Optimal design of a dragonfly-inspired compliant joint for camera positioning system of nanoindentation tester based on a hybrid integration of Jaya-ANFIS,” *Mathematical Problems in Engineering*, vol. 2018, pp. 1–17, 2018.
- [13] N. L. Chau, T. P. Dao and V. T. T. Nguyen, “An efficient hybrid approach of finite element method, artificial neural network-based multiobjective genetic algorithm for computational optimization of a linear compliant mechanism of nanoindentation tester,” *Mathematical Problems in Engineering*, vol. 2018, pp. 1–19, 2018.
- [14] T. V. T. Nguyen, N. T. Huynh, N. C. Vu, V. N. D. Kieu and S. C. Huang, “Optimizing compliant gripper mechanism design by employing an effective bi-algorithm: Fuzzy logic and ANFIS,” *Microsystem Technologies*, vol. 2021, pp. 1–29, 2021.

- [15] Z. Chen, V. T. Nguyen and N. T. Tran, "Optimum design of the volute tongue shape of a low specific speed centrifugal pump," *Journal of Electrical & Electronic Systems*, vol. 2017, pp. 1–5, 2017.
- [16] T. A. Tarray, Z. A. Ganie and B. Youssuf, "An improved mathematical model applying practicable algorithms," *Journal of Applied Science, Engineering, Technology, and Education*, vol. 1, no. 2, pp. 114–118, 2020.
- [17] J. Sadoon and B. B. Üstündağ, "Fused and modified evolutionary optimization of multiple intelligent systems using ANN, SVM approaches," *Computers, Materials & Continua*, vol. 66, no. 2, pp. 1479–1496, 2021.
- [18] A. A. Abdallah, "How can lean manufacturing lead the manufacturing sector during health pandemics such as Covid 19: A multi response optimization framework," *Computers, Materials & Continua*, vol. 66, no. 2, pp. 1397–1410, 2021.
- [19] K. Vikram, U. Ragavendran, K. Kalita, R. K. Ghadai and X. Gao, "Hybrid metamodel—NSGA-III—EDAS based optimal design of thin film coatings," *Computers, Materials & Continua*, vol. 66, no. 2, pp. 1771–1784, 2021.
- [20] A. Peng, X. Xiao and R. Yue, "Process parameter optimization for fused deposition modeling using response surface methodology combined with fuzzy inference system," *The International Journal of Advanced Manufacturing Technology*, vol. 2014, no. 73, pp. 87–100, 2014.
- [21] B. N. Turner and S. A. Gold, "A review of melt extrusion additive manufacturing processes: Materials, dimensional accuracy, and surface roughness," *Rapid Prototyping Journal*, vol. 2015, no. 21, pp. 250–261, 2015.
- [22] F. R. Jose, P. T. James and E. R. John, "Characterization of the mesostructured of-deposition acrylonitrile-butadiene-styrene materials," *Rapid Prototyping Journal*, vol. 2000, no. 6, pp. 175–186, 2000.
- [23] Antonio Armillotta, Mattia Bellotti and Marco Cavallaro, "Warping of FDM parts: Experimental tests and analytic model," *Robotics and Computer-Integrated Manufacturing*, vol. 50, pp. 140–152, 2018.
- [24] C. K. Chua, K. F. Leong and C. S. Lim, *Rapid Prototyping: Principles and Applications*, 2<sup>nd</sup> ed., Singapore: World Scientific, 2003. [Online]. Available: <https://www.worldscientific.com/worldscibooks/10.1142/5064>.
- [25] B. N. Turner and S. A. Gold, "A review of melt extrusion additive manufacturing processes: II. Materials, dimensional accuracy, and surface roughness," *Rapid Prototyping Journal*, vol. 21, no. 3, pp. 250–261, 2015.
- [26] J. F. Rodríguez, J. P. Thomas and J. E. Renaud, "Design of fused-deposition ABS components for stiffness and strength," *Journal of Mechanical Design*, vol. 2003, no. 125, pp. 545–551, 2003.
- [27] I. Gibson, D. Rosen and B. Stucker, *Introduction and Basic Principles, Additive Manufacturing Technologies: 3D Printing, Rapid Prototyping, and Direct Digital Manufacturing*, vol. 2015. New York: Springer, pp. 1–18, 2015.
- [28] O. A. Mohamed, S. H. Masood and J. L. Bhowmik, "Optimization of fused deposition modeling process parameters: A review of current research and future prospects," *Advances in Manufacturing*, vol. 2015, no. 3, pp. 42–53, 2015.
- [29] D. Annicchiarico and J. R. Alcock, "Review of factors that affect shrinkage of molded part in injection molding," *Materials and Manufacturing Processes*, vol. 2014, no. 29, pp. 662–682, 2014.
- [30] T. K. Nguyen and B. K. Lee, "Surface morphology and roughness of fused deposition modelled parts during a novel post-processing technique," in *Proc. KSPE Annual Spring Conference*, vol. 2016, pp. 50–51, 2016.
- [31] T. K. Nguyen, A. D. Pham, M. Q. Chau, X. C. Nguyen, H. A. D. Pham *et al.*, "Development and characterization of a thermoforming apparatus using axiomatic design theory and Taguchi method," *Journal of Mechanical Engineering Research and Developments*, vol. 43, no. 6, pp. 255–268, 2020.
- [32] Y. Lutfiyansyah and G. Tanjung, "Cost comparison analysis of slab structure using concrete beam and steel beam," *Journal of Applied Science, Engineering, Technology, and Education*, vol. 2, no. 1, pp. 88–96, 2020.

- [33] A. T. Munthe and A. Gafur, "Comparative analysis study of ATC-40 and SNI 1726-2012 guidelines for beam structure performance and column trans studio apartments applications using dynamic response spectrum analysis methods," *Journal of Applied Science, Engineering, Technology, and Education*, vol. 1, no. 1, pp. 46–55, 2019.
- [34] D. Essen and L. Luqyana, "Analysis and dynamic behavior of portal structure due rotating machines loads," *Journal of Applied Science, Engineering, Technology, and Education*, vol. 1, no. 2, pp. 131–140, 2020.
- [35] R. V. V. R. Murthy, K. S. R. Murthy and M. Chavali, "Design and development of instant linear gel for coal bed methane gas operations," *Journal of Applied Science, Engineering, Technology, and Education*, vol. 3, no. 2, pp. 217–223, 2020.
- [36] S. Niknamian, "Investigation on the effect of cold drawing process on mechanical properties and structure of seamless steel (Ck60) tube," *Journal of Applied Science, Engineering, Technology, and Education*, vol. 1, no. 1, pp. 13–23, 2019.
- [37] A. B. Fakhri, S. L. Mohammed, I. Khan, A. S. Sadiq, B. Alkazemi *et al.*, "Industry 4.0: Architecture and equipment revolution," *Computers, Materials & Continua*, vol. 66, no. 2, pp. 1175–1194, 2021.
- [38] T. K. Nguyen and B. K. Lee, "Post-processing of FDM parts to improve surface and thermal properties," *Rapid Prototyping Journal*, vol. 24, no. 7, pp. 1091–1100, 2018.
- [39] T. K. Nguyen and B. K. Lee, "Investigation of processing parameters in micro-thermoforming of micro-structured polystyrene film," *Journal of Mechanical Science and Technology*, vol. 33, no. 12, pp. 5669–5675, 2019.